articles

molecular pharmaceutics

RGD-Conjugated Dendrimer-Modified Gold Nanorods for *in Vivo* Tumor Targeting and Photothermal Therapy†

Zhiming Li,[‡,§,||] Peng Huang,[§,⊥] Xuejun Zhang,[*,||] Jing Lin,[#] Sen Yang,[||] Bing Liu,[⊥] Feng Gao,[⊥] Peng Xi,[‡] Qiushi Ren,[*,‡,||] and Daxiang Cui[*,||,⊥]

Institute for Laser Medicine & Biophotonics, School of Life Sciences and Biotechnology, and National Key Laboratory of Nano/Micro Fabrication Technology, Key Laboratory for Thin Film and Microfabrication of Ministry of Education, Institute of Micro-Nano Science and Technology, Shanghai Jiao Tong University, 800 Dongchuan Road, Shanghai 200240, China, Institute of Dermatology & Department of Dermatology at No. 1 Hospital, Anhui Medical University, the Key Laboratory of Gene Resource Utilization for Severe Diseases, Ministry of Education, Hefei 230032, China, and College of Chemistry, Chemical Engineering and Biotechnology, Donghua University, Shanghai 201620, China

Received May 23, 2009; Revised Manuscript Received November 2, 2009; Accepted November 5, 2009

Abstract: Successful development of safe and effective nanoprobes for tumor targeting and selective therapy is a challenging task. Although gold nanorods(GNRs) have the potential to perform such a role, the toxicity of surfactant cetyltrimethylammonium bromides (CTAB) on their surfaces limits their applications. Here, polyamidoamine dendrimer was applied to replace CTAB molecules on the surface of gold nanorods. When the resultant dendrimer-modified gold nanorods conjugated with arginine-glycine-aspartic acid (RGD) peptides, they showed highly selective targeting and destructive effects on the cancer cells and solid tumors under near-infrared laser irradiation. Also, we successfully observed the disappearance of tumors implanted in four sample mice from test group of ten. High-performance RGD-conjugated dendrimer-modified GNR nanoprobes exhibit great potential in applications such as tumor targeting, imaging, and selective photothermal therapy.

Keywords: Gold nanorods; polyamidoamine dendrimer; RGD peptide; photothermal therapy

Introduction

One of the current challenges in biomedicine is to develop safe and effective nanoprobes for tumor targeting and selective therapy.[1,2] Gold nanomaterials have been subject to intensive investigation because of their unique physical, chemical and optical properties.[3,4] For example, gold nanoshells with laser-excited tunable plasmon resonance have been exploringly employed for clinical trials for tumor imaging and photothermal tumor ablation.[5−8] In recent years, gold nanorods (GNRs) have attracted considerable attention for their unique properties in photothermal therapy,[9−11] biosensing,[12] molecular imaging,[13] and gene delivery[14] for cancer therapy.

Although GNRs exhibit promising results in cellular imaging, spectral detection and photoactivated therapy, there are still some concerns remaining about synthesis, surface modifications, biocompatibility and toxicity.[15] For example, the toxicity derived from a large amount of the surfactant

* Corresponding authors. E-mail: zhangxj@ahmu.edu.cn; qsren@sjtu.edu.cn; dxcui@sjtu.edu.cn. Mailing address (D.C.): Shanghai Jiao Tong University, Department of Bio-Nano Science and Engineering, 800 Dongchuan Road, Shanghai 200240, China. Tel: 86-21-34206886, Fax: 86-21-34206886.

† Competing interests statement: The authors declare that they have no competing financial interests.

‡ Institute for Laser Medicine & Biophotonics, School of Life Sciences and Biotechnology, Shanghai Jiao Tong University.

§ Identical contribution to this paper.

|| Anhui Medical University.

⊥ National Key Laboratory of Nano/Micro Fabrication Technology, Key Laboratory for Thin Film and Microfabrication of Ministry of Education, Institute of Micro-Nano Science and Technology, Shanghai Jiao Tong University.

Donghua University.

10.1021/mp9001415
Published on Web 11/05/2009

cetyltrimethylammonium bromide (CTAB) during GNR synthesis severely limits their biomedical applications. Several methods have been employed to remove CTAB molecules on the surface of GNRs.[16−21] However, the complete removal of CTAB molecules on the surface of GNRs is difficult to achieve. Therefore, developing a new method to replace CTAB molecules on the surface of GNRs is critical to improve their biocompatibility and enhance their potential applications in *in vivo* imaging and photothermal therapy.

Dendrimers are a class of polymers with highly ordered structure. The accretion of functional groups, symmetry perfection, nanosize, and internal cavities provide these dendritic nanocomposites many potential applications in nanomedicine.[22,23] Dendrimer coatings of nanoparticle surfaces can alter the charge, functionality, and reactivity, as well as enhance the stability and dispersion of the nanoparticles.[24] Our previous results demonstrated that dendrimer-functionalized nanomaterials, such as carbon nanotubes, quantum dots and magnetic nanoparticles, markedly enhance the biocompatibility and cellular uptake of nanoparticles.[25−28] So far no report is closely associated with the biocompatibility of dendrimer-modified GNRs and tumor targeting therapy based on dendrimer-modified GNRs.

Integrin $\alpha_V\beta_3$, an important biomarker overexpressed in sprouting tumor vessels and most tumor cells, plays a critical role in regulating tumor growth, metastasis and tumor angiogenesis.[29,30] The RGD (arginine-glycine-aspartic acid) short peptides can specifically bind with integrin $\alpha_V\beta_3$,[31] and RGD-conjugated quantum dots have been successfully employed for tumor imaging,[32] thus we selected the RGD peptides as the targeting molecules for melanoma targeting and selective therapy.

(1) Nie, S.; Xing, Y.; Kim, G.; Simons, J. Nanotechnology applications in cancer. *Annu. Rev. Biomed. Eng.* **2007**, *9*, 257–288.

(2) Qian, X.; Peng, X.; Ansari, D.; Yin-Goen, Q.; Chen, G.; Shin, D.; Yang, L.; Young, A.; Wang, M.; Nie, S. In vivo tumor targeting and spectroscopic detection with surface-enhanced Raman nanoparticle tags. *Nat. Biotechnol.* **2008**, *26*, 83–90.

(3) Huang, X.; Jain, P.; El-Sayed, I.; El-Sayed, M. Gold nanoparticles: interesting optical properties and recent applications in cancer diagnostics and therapy. *Nanomedicine* **2007**, *2*, 681–693.

(4) Yang, D.; Cui, D. Advances and prospects of gold nanorods. *Chem. Asian J.* **2008**, *3*, 2010–2022.

(5) Hirsch, L.; Stafford, R.; Bankson, J.; Sershen, S.; Rivera, B.; Price, R.; Hazle, J.; Halas, N.; West, J. Nanoshell-mediated near-infrared thermal therapy of tumors under magnetic resonance guidance. *Proc. Natl. Acad. Sci. U.S.A.* **2003**, *100*, 13549–13554.

(6) Loo, C.; Lowery, A.; Halas, N.; West, J.; Drezek, R. Immunotargeted nanoshells for integrated cancer imaging and therapy. *Nano Lett.* **2005**, *5*, 709–711.

(7) Gobin, A.; Lee, M.; Halas, N.; James, W.; Drezek, R.; West, J. Near-infrared resonant nanoshells for combined optical imaging and photothermal cancer therapy. *Nano Lett.* **2007**, *7*, 1929–1934.

(8) Loo, C.; Hirsch, L.; Lee, M.; Chang, E.; West, J.; Halas, N.; Drezek, R. Gold nanoshell bioconjugates for molecular imaging in living cells. *Opt. Lett.* **2005**, *30*, 1012–1014.

(9) Huang, X.; El-Sayed, I.; Qian, W.; El-Sayed, M. Cancer cell imaging and photothermal therapy in the near-infrared region by using gold nanorods. *J. Am. Chem. Soc.* **2006**, *128*, 2115–2120.

(10) Huff, T.; Tong, L.; Zhao, Y.; Hansen, M.; Cheng, J.; Wei, A. Hyperthermic effects of gold nanorods on tumor cells. *Nanomedicine* **2007**, *2*, 125–132.

(11) Tong, L.; Zhao, Y.; Huff, T.; Hansen, M.; Wei, A.; Cheng, J. Gold Nanorods Mediate Tumor Cell Death by Compromising Membrane Integrity. *Adv. Mater.* **2007**, *19*, 3136–3141.

(12) Wang, C. G.; Chen, Y.; Wang, T. T.; Ma, Z. F.; Su, Z. M. Monodispersed Gold nanorod-embedded silica particles as novel raman labels for biosensing. *Adv. Funct. Mater.* **2008**, *18*, 355–361.

(13) Von Maltzahn, G.; Centrone, A.; Park, J.; Ramanathan, R.; Sailor, M.; Hatton, T.; Bhatia, S. SERS-Coded Gold Nanorods as a Multifunctional Platform for Densely Multiplexed Near-Infrared Imaging and Photothermal Heating. *Adv. Mater.* **2009**, *21*, 1–6.

(14) Chen, C.; Lin, Y.; Wang, C.; Tzeng, H.; Wu, C.; Chen, Y.; Chen, C.; Chen, L.; Wu, Y. DNA-gold nanorod conjugates for remote control of localized gene expression by near infrared irradiation. *J. Am. Chem. Soc.* **2006**, *128*, 3709–3715.

(15) Eghtedari, M.; Liopo, A.; Copland, J.; Oraevsky, A.; Motamedi, M. Engineering of hetero-functional gold nanorods for the in vivo molecular targeting of breast cancer cells. *Nano Lett.* **2009**, *9*, 287–291.

(16) Huang, X.; El-Sayed, I.; Qian, W.; El-Sayed, M. Cancer cells assemble and align gold nanorods conjugated to antibodies to produce highly enhanced, sharp, and polarized surface Raman spectra: a potential cancer diagnostic marker. *Nano Lett.* **2007**, *7*, 1591–1597.

(17) Takahashi, H.; Niidome, Y.; Niidome, T.; Kaneko, K.; Kawasaki, H.; Yamada, S. Modification of gold nanorods using phosphatidylcholine to reduce cytotoxicity. *Langmuir* **2006**, *22*, 2–5.

(18) Niidome, Y.; Honda, K.; Higashimoto, K.; Kawazumi, H.; Yamada, S.; Nakashima, N.; Sasaki, Y.; Ishida, Y.; Kikuchi, J. Surface modification of gold nanorods with synthetic cationic lipids. *Chem. Commun. (Cambridge)* **2007**, *28*, 3777–3779.

(19) Niidome, T.; Yamagata, M.; Okamoto, Y.; Akiyama, Y.; Takahashi, H.; Kawano, T.; Katayama, Y.; Niidome, Y. PEG-modified gold nanorods with a stealth character for in vivo applications. *J. Controlled Release* **2006**, *114*, 343–347.

(20) Wijaya, A.; Hamad-Schifferli, K. Ligand customization and DNA functionalization of gold nanorods via round-trip phase transfer ligand exchange. *Langmuir* **2008**, *24*, 9966–9969.

(21) Orendorff, C.; Alam, T.; Sasaki, D.; Bunker, B.; Voigt, J. Phospholipid-gold nanorod composites. *ACS Nano* **2009**, *3*, 971–983.

(22) Frechet, J. Dendrimers and other dendritic macromolecules: From building blocks to functional assemblies in nanoscience and nanotechnology. *J. Polym. Sci., Part A: Polym. Chem.* **2003**, *41*, 3713–3725.

(23) Lee, C.; MacKay, J.; Fréchet, J.; Szoka, F. Designing dendrimers for biological applications. *Nat. Biotechnol.* **2005**, *23*, 1517–1526.

(24) Shan, J.; Tenhu, H. Recent advances in polymer protected gold nanoparticles: synthesis, properties and applications. *Chem. Commun. (Cambridge)* **2007**, *44*, 4580–4598.

(25) Li, Z.; Huang, P.; Lin, J.; He, R.; Liu, B.; Zhang, X.; Yang, S.; Xi, P.; Zhang, X.; Ren, Q.; Cui, D. Arginine-Glycine-Aspartic Acid-Conjugated Dendrimer-Modified Quantum Dots for Targeting and Imaging Melanoma. *J. Nanosci. Nanotechnol.* **2010**, *10*, 1–9.

(26) Pan, B.; Cui, D.; Xu, P.; Ozkan, C.; Feng, G.; Ozkan, M.; Huang, T.; Chu, B.; Li, Q.; He, R. Synthesis and characterization of polyamidoamine dendrimer-coated multi-walled carbon nanotubes and their application in gene delivery systems. *Nanotechnology* **2009**, *20*, 125101.

(27) Pan, B.; Gao, F.; Ao, L.; Tian, H.; He, R.; Cui, D. Controlled self-assembly of thiol-terminated poly(amidoamine) dendrimer and gold nanoparticles. *Colloids Surf., A* **2005**, *259*, 89–94.

Here we report that a class of safe and effective nanoprobes, RGD-conjugated dendrimer-modified gold nanorods (RGD-dGNRs), was employed for *in vivo* tumor targeting and selective photothermal therapy. First, we used the partially thiolated polyamidoamine (PAMAM) dendrimer to replace CTAB molecules on the surface of GNRs, with the aim of improving the biocompatibility of prepared GNRs. Then, we prepared unique tumor targeting nanoprobes by conjugating dendrimer-modified GNRs with RGD peptides, and identified their maximal absorption peak around 820 nm. Finally we investigated the feasibility of prepared nanoprobes for tumor targeting and photothermal therapy *in vitro* and *in vivo* under near-infrared laser irradiation (NIR) on xenograft tumor model. We found that the prepared nanoprobes can selectively kill tumor cells *in vitro* and *in vivo*, and extend the lifespan of mice loaded with tumors.

Experimental Section

Synthesis and Characterization of RGD-dGNR Nanoprobes. GNRs were synthesized according to the seed-mediated template-assisted protocol and our previous reports.[33,34] Functional PAMAM dendrimers, with a small number of thiol groups, were prepared by reacting G4.0 PAMAM dendrimers with methyl mercaptoacetate.[25,27] The degree of thiolation and purity of thiolated G4.0 dendrimer were monitored using ^{1}H nuclear magnetic resonance (^{1}H NMR) analysis. Then ligand exchange was utilized to remove CTAB molecules on the surface of GNRs by the way of the phase transfer procedure.[20] Those amine groups on the surface of dendrimer-covered GNRs were converted to carboxylic acids by reacting with excess glutaric anhydride, then conjugated with RGD (Supplementary Figure 8a in the Supporting Information).[35] Prepared RGD-dGNR nanoprobes were characterized by HR-TEM (Hitachi H-700H), AFM (Veeco Instruments Inc.), ^{1}H NMR (Bruker Avance III 400), TGA (TA Instruments) and UV−vis absorbance spectroscopy.

Cell Targeting of RGD-dGNR Nanoprobes. The MCF-7 cell line with lower expression of $\alpha_V\beta_3$ was selected as the negative control group. HUVEC cell line with overexpression of $\alpha_V\beta_3$ was used as positive control group. The melanoma A375 cell line with overexpression of $\alpha_V\beta_3$ was selected as the test group. The expression of $\alpha_V\beta_3$ in tumor cells was determined by flow cytometry (FCM). The three kinds of cells were cultured in DMEM medium supplemented with 10% FBS and 1% penicillin−streptomycin in a humidified 5% CO_2 balanced air incubator at 37 °C for 2 days. All the cells were collected and implanted onto 18 mm glass coverslips in a 12-well tissue culture plate, and culturing was continued for 3 days. After the cells were rinsed 3 times, 500 μL of medium containing prepared nanoprobes was added into each dish and incubated for 30 min. Subsequently, these cells were rinsed with PBS buffer, fixed with 4% paraformaldehyde, coated with glycerol, and sealed with another coverslip. Then these cells were imaged by dark field microscope under a reflective mode (Zeiss Axioscope). Parallel competition inhibition control experiments were set up. Before A375 cells were incubated with RGD-dGNR nanoprobes, these cells were first incubated with free RGD peptides, then incubated with RGD-dGNR nanoprobes, then washed with PBS buffer, and then examined under the dark field microscope. Finally these cells were made into TEM specimens, and were observed by HR-TEM.

Cytotoxicity and Selective Photothermal Therapy of dGNRs. The Cell Counting Kit-8 assay (Dojindo Laboratories) was used to measure cytotoxicity of synthesized nanoprobes following the instruction of the kit. Cells incubated with and without RGD-dGNR nanoprobes were exposed to NIR laser irradiation, with a wavelength of 808 nm and varying intensities, from 30 mW (4 W/cm^2) to 150 mW (20 W/cm^2) in increments of 40 mW. The laser spot size is 1.0 mm in diameter, and the exposure time is 4 min. The cell viability was tested by both 0.4% trypan blue and Calcein-AM staining.

Distribution and Selective Photothermal Therapy of Nanoprobes. Animal experiments were performed according to Guidelines for Animal Care and Use Committee, Shanghai Jiao Tong University. Melanoma A375 cells (5×10^6) were injected subcutaneously into the right rear flank area of 50 female nude mice of age 6 to 8 weeks. When tumors grew to 5 mm in diameter, 200 μg of RGD-dGNR nanoprobes was injected into mice via tail vein. For the blocking experiment, ten mice were injected with the mixture of 0.5 mg of RGD peptides and 200 μg of RGD-dGNR nanoprobes. For passive targeting experiment, 200 μg of pure dGNRs was injected into ten nude mice via tail vein. Mice were respectively sacrificed at 3 h, 6 h, 9 h, and 12 h. Blood and organs were collected and kept in liquid nitrogen. Blood and tissue samples were lysed in aqua regia. The precipitates were dissolved in 0.5 M HCl, the amount of RGD-dGNRs was measured by inductively coupled plasma mass spectrometry (Thermo, U.K.).

(33) Pan, B.; Ao, L.; Gao, F.; Tian, H.; He, R.; Cui, D. End-to-end self-assembly and colorimetric characterization of gold nanorods and nanospheres via oligonucleotide hybridization. *Nanotechnology* **2005**, *16*, 1776–1780.
(34) Murphy, C.; Jana, N. Controlling the aspect ratio of inorganic nanorods and nanowires. *Adv. Mater.* **2002**, *14*, 80–82.
(28) Pan, B.; Cui, D.; Sheng, Y.; Ozkan, C.; Gao, F.; He, R.; Li, Q.; Xu, P.; Huang, T. Dendrimer-modified magnetic nanoparticles enhance efficiency of gene delivery system. *Cancer Res.* **2007**, *67*, 8156–8163.
(29) Allman, R.; Cowburn, P.; Mason, M. In vitro and in vivo effects of a cyclic peptide with affinity for the alpha(nu)beta3 integrin in human melanoma cells. *Eur. J. Cancer* **2000**, *36*, 410–422.
(30) Hood, J.; Cheresh, D. Role of integrins in cell invasion and migration. *Nat. Rev. Cancer* **2002**, *2*, 91–100.
(31) Pierschbacher, M.; Ruoslahti, E. Cell attachment activity of fibronectin can be duplicated by small synthetic fragments of the molecule. *Nature* **1984**, *309*, 30–33.
(32) Cai, W.; Chen, X. Preparation of peptide-conjugated quantum dots for tumor vasculature-targeted imaging. *Nat. Protoc.* **2008**, *3*, 89–96.
(35) Shukla, R.; Thomas, T.; Peters, J.; Kotlyar, A.; Myc, A.; Baker, J. Tumor angiogenic vasculature targeting with PAMAM dendrimer-RGD conjugates. *Chem. Commun. (Cambridge)* **2005**, *46*, 5739–5741.

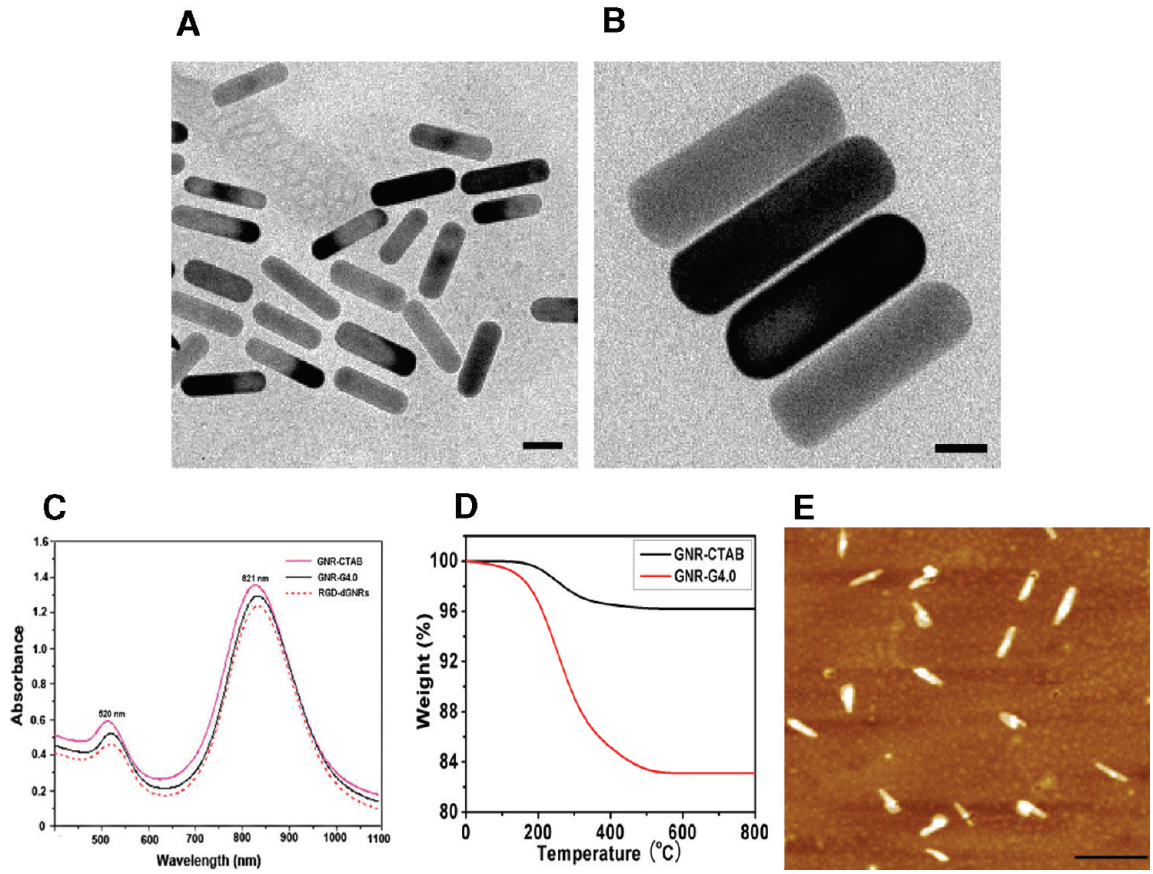

Figure 1. Characterization of CTAB-GNRs and RGD-dGNRs. (A) High resolution transmission electron microscopy (HR-TEM) images of GNR-CTAB, scale bar, 20 nm. (B) HR-TEM images of GNR-G4.0, scale bar, 10 nm. (C) UV−vis absorbance spectra of GNRs before and after dendrimer modification and RGD peptide conjugation. (D) TGA curves showing difference in the weight loss of GNR-G4.0 and CTAB-GNRs. (E) AFM images of RGD-dGNRs deposited on a silicon wafer. This image covers a 5 μm $\times$ 5 μm area and was obtained with a Digital Instruments Multimode AFM operated in air using a tapping mode, scale bar, 100 nm.

Mice loaded with tumors were randomly divided into four groups: test group (10 mice) (200 μg of nanoprobes plus NIR laser irradiation); sham control group (10 mice) (PBS plus NIR laser irradiation), and blank control (10 mice) (untreated) as well as passive targeting group (10 mice) (200 μg of dGNRs plus NIR laser irradiation). When the tumor sizes reached about 5 mm in diameter, the nude mice were injected with 200 μg of prepared nanoprobes in PBS via tail vein. At 6 h after injection, the mice were anesthetized and irradiated with a NIR laser with a wavelength of 808 nm at a power density of 24 W/cm^2 and a spot size of 5 mm diameter for 5 min. Tumors were irradiated for four times per month, once every week.

Observation by Real Time Reflectance Confocal Microscopy. Real time reflectance confocal micrscopy (RCM) was used to collect images of tumors from test group and control group at 3 h, 1 day and 7 weeks after nanoprobes injection, and to assess the histological and blood flow changes. Hematoxylin and eosin staining was used to examine tumor histological changes. Tumor size and mice survivability were monitored for 7 weeks.

Statistical Analyses. All data are presented in this paper as mean result $\pm$ SD. Statistical differences were evaluated using the t test and considered significant at the $P < 0.05$ level. All figures shown in this article were obtained from three independent experiments with similar results. Median survival times were computed by using Kaplan−Meier methods. 95% confidence intervals were computed. Differences in survival functions were assessed using the log rank test. All analyses were performed using SPSS 14.0 software.

Results

Development of RGD-Conjugated dGNR Nanoprobes. As shown in Supplementary Figure 1 in the Supporting Information, the main route for GNR ligand exchange is as follows: gold nanorods with CTAB first were synthesized, then partially thiolated G4.0 PAMAM dendrimers were prepared, and then the thiolated G4.0 PAMAM dendrimers were used to replace CTAB molecules on the surface of gold nanorods; the resultant G4.0 dendrimer-modified GNRs (dGNRs) were conjugated with RGD peptides (RGD-dGNRs). The original gold nanorods (GNRs-CTAB) are about 42 nm in length, and 10 nm in width (Figure 1a).

Dendrimer-modified GNRs exhibit better dispersion in water solution than GNRs-CTAB (Figure 1b). GNRs-CTAB has two absorption bands, a weak short-wavelength band around 520 nm and a strong long-wavelength band around 821 nm. RGD-dGNRs exhibit an absorption band red-shift (about 3 nm) (Figure 1c). We observed that RGD-dGNRs exhibited good stability and dispersibility in water or organic solution with different pH conditions (Supplementary Figure 2 in the Supporting Information).

We also used thermal gravimetric analysis (TGA) to calculate the content (%) of the CTAB-modified GNRs and G4.0-dendrimer-modified GNRs. The CTAB layer on the surface of GNRs has ~4% weight loss, while G4.0-dendrimer-modified GNRs have a ~17% weight loss (Figure 1d). Atomic force microscopy (AFM) images revealed discrete entities with a dendrimer layer. Cross section of height analysis of these entities revealed vertical heights of 15 to 20 nm. The uniform appearance and height values of these entities demonstrated that these structures are a single RGD-dGNR. The lateral size of a single RGD-dGNR is about 51 to 55 nm, which fits well with the predicted size (diameter of G4.0 is about 4.5 nm). Therefore, CTAB molecules on the surface of gold nanorods were completely replaced by dendrimer, and prepared RGD-dGNRs exhibited good dispersibility in water solution (Figure 1e).

Evaluation of RGD-dGNR Nanoprobes for *in Vitro* Tumor Cell Targeting. FCM analysis indicated the melanoma A375 cell lines and normal human umbilical vein endothelial (HUVEC) cells exhibit overexpression of $\alpha_V\beta_3$ integrin, and the breast cancer cell line MCF-7 cells exhibit lower expression of $\alpha_V\beta_3$ integrin (Supplementary Figure 3 in the Supporting Information). Initial evaluation of the cytotoxicity of RGD-dGNR nanoprobes (Supplementary Figure 4 in the Supporting Information) showed both the dendrimer-modified GNRs and RGD-dendrimer-modified GNRs were biologically nontoxic within the concentration of ~200 μg/mL. GNR-CTAB concentration of ~200 μg/mL exhibited marked cytotoxicity.

Then we evaluated the specificity and sensitivity of RGD-dGNR nanoprobes for tumor cell targeting. Under dark field microscopy, melanoma A375 cells incubated with RGD-dGNR nanoprobes (Figure 2A2) exhibit a strong golden color; the melanoma A375 cells incubated with dGNRs (Figure 2B2 and C2) and preincubated with free RGD peptides did not exhibit a golden color, and similar negative results also were observed for MCF-7 cells incubated with dGNRs or RGD-dGNRs, which highly suggests that free RGD peptides can block the binding of RGD-dGNR nanoprobes with $\alpha_V\beta_3$ integrins overexpressed in the tumor cells, and RGD-dGNR nanoprobes can specifically target melanoma A375 cells. The sensitivity of prepared nanoprobes for targeting melanoma A375 cells is 0.5 μg/mL or so. Further observation showed that the RGD-dGNR nanoprobes were located both on the surface and in the cytoplasm of melanoma A375 cells after incubation of melanoma A375 cells with prepared nanoprobes for 24 h (Figure 2D1 and D2).

Selective Photothermal Therapy of Tumor Cells Incubated with RGD-dGNR Nanoprobes. A375 cells incubated with RGD-dGNR nanoprobes exhibited destruction within the laser spots after exposure to the laser at 70 mW (Figure 3A1). When the laser energy reached 110 mW, the amount of destroyed tumor cells increased accordingly (Figure 3A4). Few damaged cells were observed for the A375 cells treated with dGNRs or NIR light alone (Figures 3A2, 3A3, 3A5, and 3A6). Similarly, no dead cells were observed for MCF-7 cells treated with RGD-dGNR nanoprobes, pure GNRs, or NIR laser irradiation. These results fully showed that RGD-dGNR nanoprobes were only employed to kill cancer cells with overexpression of $\alpha_V\beta_3$ integrin under NIR irradiation. Therefore, the prepared RGD-dGNR nanoprobes have the capability of selective photothermal therapy on the cancer cells.

Under the condition of 110 mW laser irradiation for 4 min, as the amount of RGD-dGNR nanoprobes in the medium increased, the amount of destroyed cells also increased accordingly. When the concentration of RGD-dGNR nanoprobes in the medium reached 100 μg/mL, all cancer cells were killed within the laser spots (Figure 3B3). Therefore, 100 μg/mL RGD-dGNR nanoprobes was considered as the optimal photothermal therapeutic concentration for *in vitro* cancer cells.

***In Vivo* Tumor Photothermal Therapy.** Mouse models loaded with melanoma A375 cells were established (Figure 4a). The distribution of RGD-dGNR nanoprobes was examined in the whole body of mouse models, which showed that 47% of the injected RGD-dGNR nanoprobes located in the blood at 3 h after injection, 17% of the RGD-dGNR nanoprobes accumulated in local tumor tissues at 6 h after injection (Figure 4b), and nanoprobes in the blood decreased gradually in a time-dependent manner. Nanoprobes in the tumor tissues increased gradually as time increased, which fully suggests that the prepared RGD-dGNR nanoprobes were targeting tumor tissues. Six hours after injection was selected as the optimal time to begin the NIR laser irradiation on the tumor locations in the control group or test group. For the competition inhibition experiment group, few RGD-dGNR nanoprobes accumulated in the tumor location (Supplementary Figure 5 in the Supporting Information), highly indicating the free RGD peptides can first bind with $\alpha_V\beta_3$ integrin on the surface of tumor cells, and block the specific binding of RGD-dGNR nanoprobes with the tumor cells and vasculature endothelial cells *in vivo*, finally resulting in the failure of *in vivo* photothermal therapy.

For the passive targeting group, partial dGNRs were observed to accumulate in tumor sites (Supplementary Figure 6 in the Supporting Information), indicating dendrimer-modified GNRs can preferentially accumulate in the tumor tissues due to the EPR (enhanced permeability and retention) effects. However, compared with the test group, the amount of dGNRs in tumor locations was less than that in the test group.

Under the NIR laser irradiation, the average tumor size in the test group was markedly smaller than those in the control

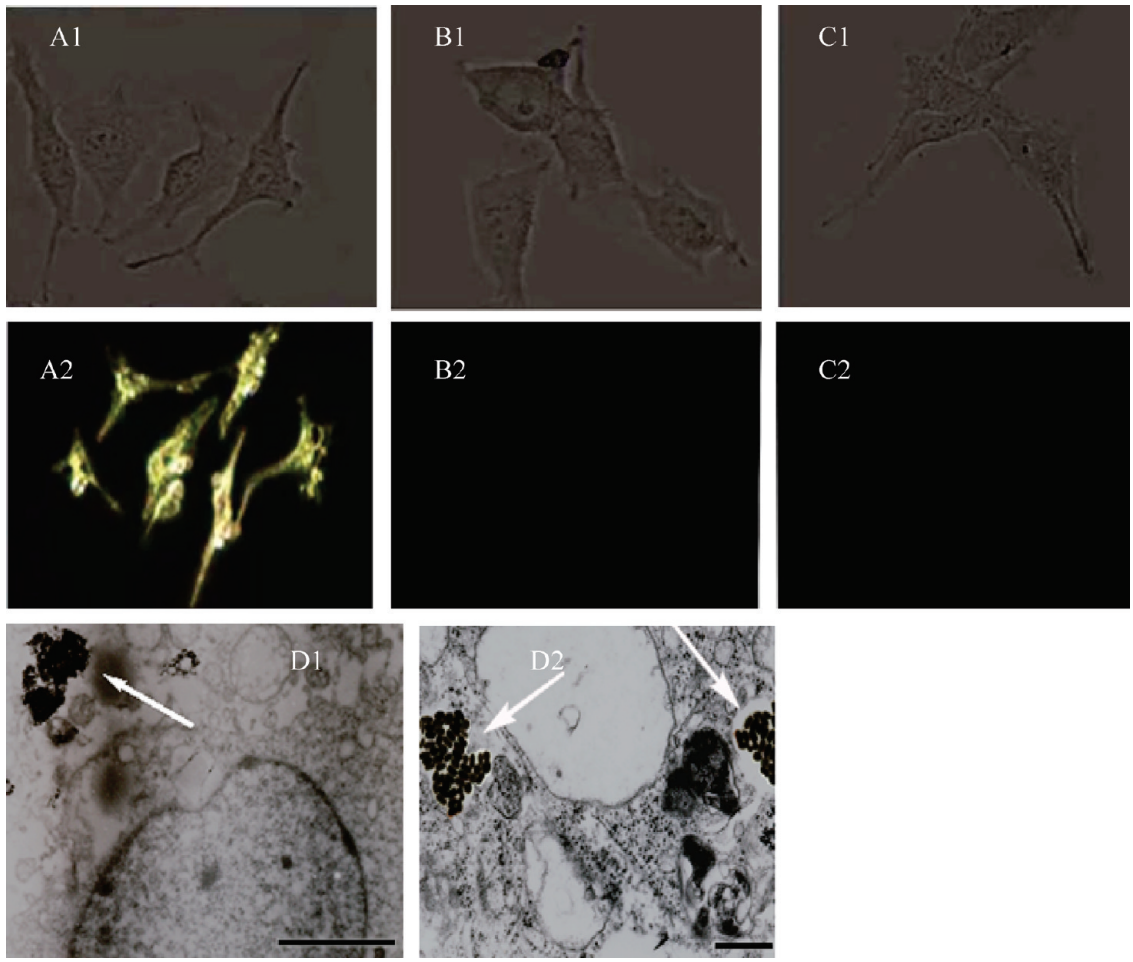

Figure 2. Light scattering images and intracellular location of RGD-dGNRs. Reflective mode dark-field images and bright field images of RGD-dGNRs (A), dGNRs (B), and free peptide and RGD-dGNRs (C) after incubation with A375 cells for 30 min at room temperature. The images were acquired with a Zeiss Axioscope2 microscope imaging system. A1: bright field image of A375 cells incubated with RGD-dGNRs exhibiting cell shapes. A2: dark-field image of melanoma A375 cells incubated with RGD-dGNR nanoprobes, exhibiting golden color. B1: bright field image of A375 cells incubated with dGNRs exhibiting cell shapes. B2: dark-field image of melanoma A375 cells incubated with RGD-dGNR nanoprobes, exhibiting black color. C1: bright field image of A375 cells incubated with free peptite and RGD-dGNRs, exhibiting cell shapes. C2: dark-field image of melanoma A375 cells incubated with free peptite and RGD-dGNRs, exhibiting black color. (D1 and D2) TEM images of RGD-dGNRs (arrow) in cytoplasm of melanoma A 375 cells, left scale bar, 500 nm; right scale bar, 200 nm.

groups (Figure 4c). As the laser irradiation times and mouse breeding time increased, the tumors became smaller and smaller. Conversely, the tumors in the control groups grew bigger and bigger. Interestingly, we observed, the tumor tissues in four mice almost completely disappeared in three weeks or so. In addition, passive targeting photothermal therapy based on dGNRs can also slightly inhibit tumor growth, which is consistent with biodistribution of dGNRs in tumor tissues. However, compared with active selective tumor ablation based on RGD-dGNR nanoprobes, passive targeting therapy based on dGNRs exhibits lower efficiencies ($p < 0.05$) (Supplementary Figure 7 in the Supporting Information).

Regarding the effects of nanoprobes plus NIR laser irradiation on the longevity of mice loaded with tumors, we observed that the median survivability of mice in the control group without any treatment was three weeks, in the control group treated with PBS plus NIR laser was four weeks, and in the test group was more than seven weeks. The survivability of mice in the test group was markedly stronger than the one in the control group, $P = 0.006$. The Kaplan−Meier curve suggests that the therapy based on nanoprobe injection plus NIR laser irradiation can markedly increase the survival time of mice with tumors (Figure 4d).

The potential mechanism of RGD-dGNR nanoprobe-based photothermal therapy was also investigated by using real time reflectance confocal microscopy (RCM). We observed that the blood flow inside tumor tissues in the test group began to be blocked at 3 h after NIR laser irradiation (Supplementary Video 1 in the Supporting Information). In the control group, no obvious dynamic blood flow alteration was observed. Additionally, after seven weeks of treatment, RCM images of tumors in the test group clearly displayed numerous gossamer-like collagen bundles and branchlike

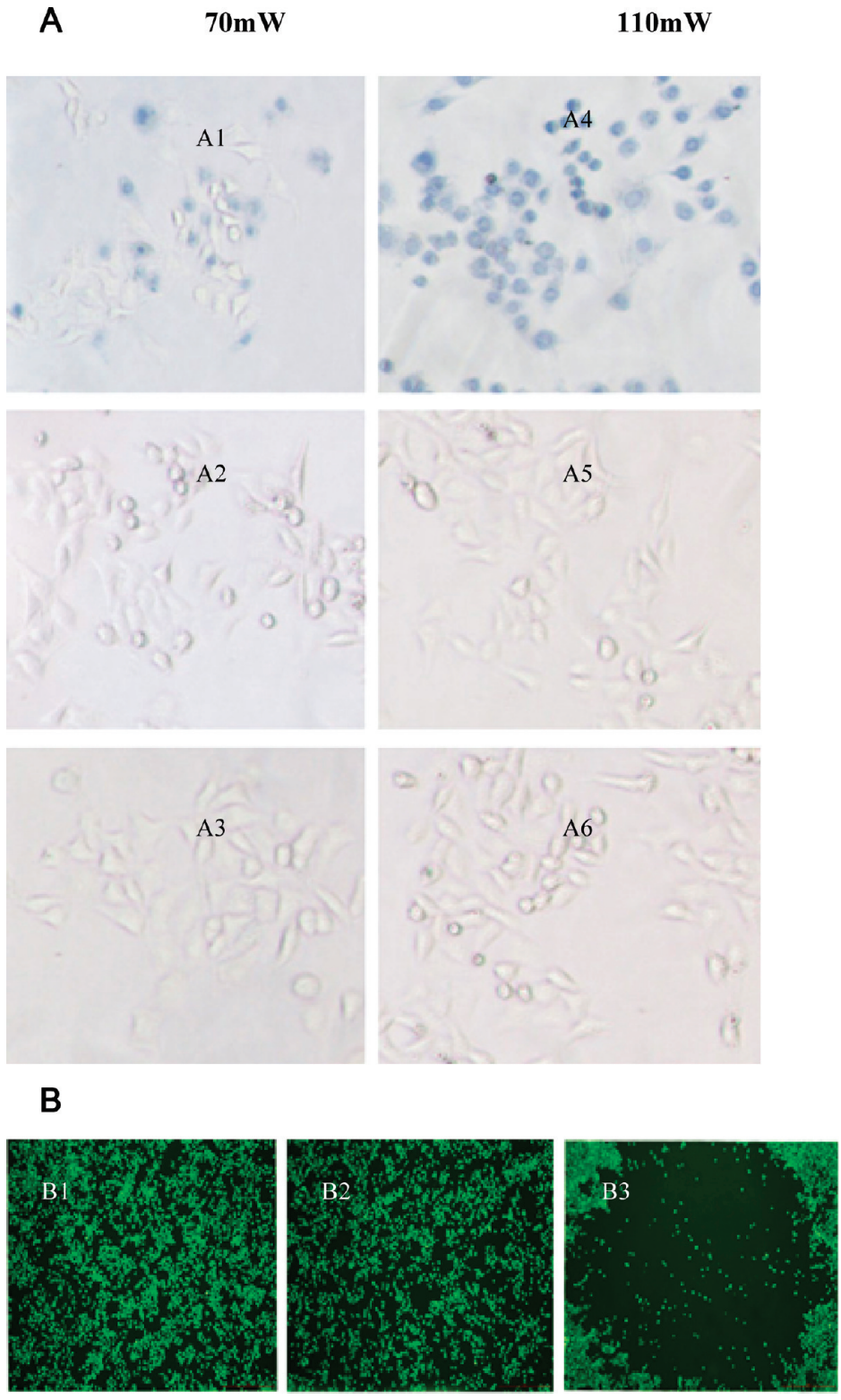

Figure 3. Selective destruction of A375 cancer cells incubated with RGD-dGNR nanoprobes. (A) Cell death analysis via trypan blue staining. A1: partial cell death exhibiting blue color under 70 mW laser irradiation in the test group with RGD-dGNRs plus irradiation. A2: no dead cells in the control group with pure GNRs. A3: no dead cells in the control group with NIR irradiation. A4: all cell death exhibiting blue color under 110 mW laser irradiation. A5: no dead cells in the control group with pur GNRs. A6: no dead cells in the control group with NIR irradiation. (B) Cell viability assessed via calcein staining. B1: no dead cells in the test group with 0.1 μg/mL RGD-dGNRs. B2: no dead cells in the test group with 5 μg/mL RGD-dGNRs. B3: cell death and disappearance within the spot in test group with 100 μg/mL RGD-dGNRs.

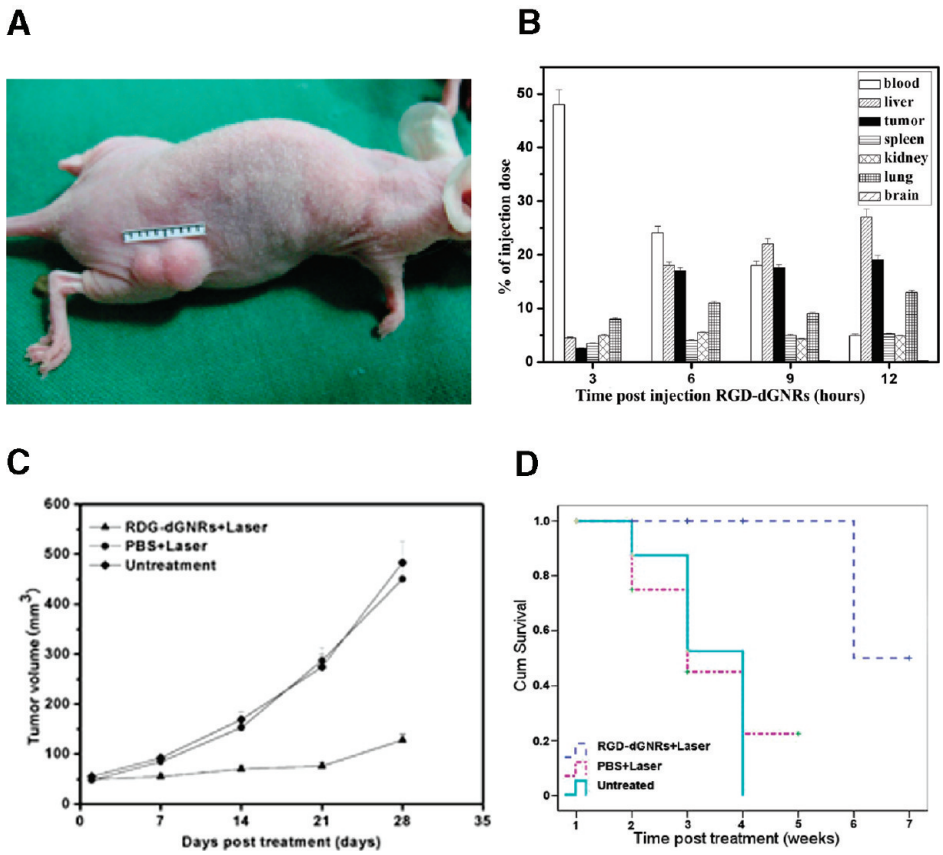

Figure 4. Melanoma animal models, biodistribution of RGD-dGNRs, and survival data analysis of control and test group. (A) A375 melanoma mouse models. The tumor size can be calculated as $ab^2/2$ (a represents the longer dimension and b represents the shorter dimension of the tumor). (B) Biodistribution of RGD-dGNRs in mice after intravenous injection. Several time points after injection, gold amounts in tissue samples were evaluated by ICP mass spectrometry ($n = 3$). (C) Tumor size at different time points postirradiation of mice treated with RGD-dGNRs plus NIR laser (group 1); PBS plus NIR laser (group 2) or untreated control (group 3), $P < 0.05$ for group 2 or group 3 versus group 1. (D) Kaplan−Meier curve of the test group and control group, $P = 0.006$.

collagens (white arrow) (Figure 5A1). Numerous reflective melanoma cells (white arrow) were still distributed throughout the tumor tissues in the control group; some similar cells in morphology and refractivity existed in a low density and spare cluster (Figures 5A2 and 5A3). Accordingly, histological analysis showed that the tumors in test group after seven weeks of treatment exhibited a scarlike structure containing numerous collagen bundles (Figure 5B1). A lot of tumor cells were observed in those tumors untreated (Figure 5B3) and treated with the PBS plus laser irradiation (Figure 5B2).

All data mentioned above confirmed that RGD-dGNR nanoprobes own active targeting abilities and, under NIR laser irradiation, exhibit selective destructive effects on targeted cancer cells.

Discussion

Gold nanorods, due to their strong light enhanced absorption in NIR regions and plasmon resonance enhanced properties, have become a class of promising candidates for tumor targeting and selective therapy.[3,4] Due to the toxicity caused by CTAB molecules on the surface of GNRs, GNR-based tumor targeting and photothermal therapy has not been successfully achieved in animals loaded with tumors to date. Although PEGylated gold nanorods have been investigated for their applications in photothermal therapeutics in mice loaded with tumors,[36] this kind of passive targeting therapy is based on the preferential accumulation of nanoparticles in local tumors due to the EPR effects, and cannot realize specific tumor targeting therapy. Therefore, to develop safe and effective GNR-based nanoprobes for active tumor targeting therapy is very necessary.

In this study, successful use of dendrimer to replace CTAB molecules on the surface of GNRs markedly enhanced the biocompatibility of gold nanorods. TGA and cytotoxicity evaluation of prepared RGD-dGNRs fully suggest that CTAB molecules on the surface of GNRs were completely replaced by dendrimer. Positive development of the RGD-dGNR nanoprobe-based active tumor targeting therapy was accomplished. Our results demonstrated that RGD markedly

(36) Dickerson, E. B.; Dreaden, E. C.; Huang, X; El-Sayed, I. H.; Chu, H; Pushpanketh, S.; McDonald, J. F.; El-Sayed, M. A. Gold nanorod assisted near-infrared plasmonic photothermal therapy (PPTT) of squamous cell carcinoma in mice. *Cancer Lett.* **2008**, *269*, 57–66.

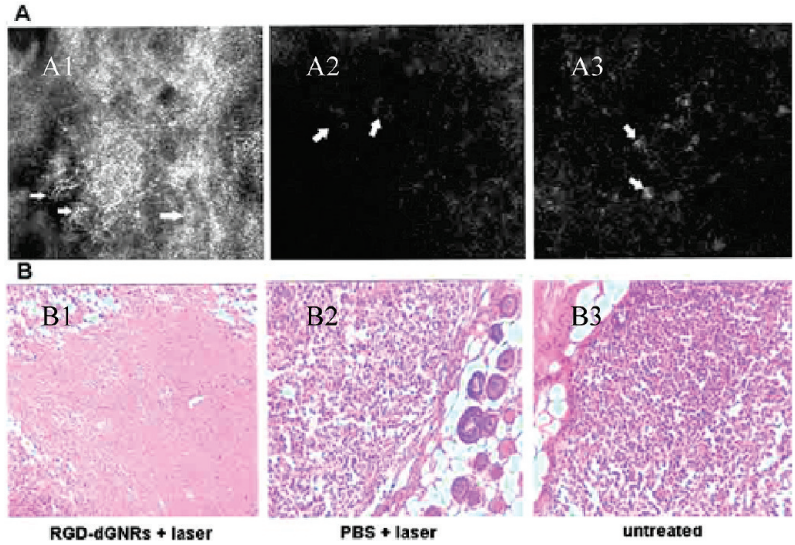

Figure 5. RCM images and histological images of tumor seven weeks after treatment. (A) RCM images (0.25 mm × 0.25 mm) of tumor were acquired with Vivascope 3000 microscopes (Lucid) using a diode laser with a wavelength of 830 nm and a 30× objective lens of numerical aperture (NA) 0.9 (water immersion). A1: Arrows indicate numerous gossamer-like collagen bundles and branchlike collagens. A2 and A3: arrows indicate that some reflective melanoma cells existed in a low density and spare cluster. (B) Corresponding histological images (20×) of tumor using hematoxylin and eosin staining in the group of RGD-dGNRs plus laser irradiation (B1), group of PBS plus laser irradiation (B2) and the untreated control group (B3). B1: a scarlike structure containing numerous collagen bundles in the tumor location. B2: a lot of tumor cells existed. B3: a lot of tumor cells existed.

enhanced the tumor targeting of dGNRs, and prepared RGD-dGNR nanoprobes can target and destroy tumor cells with overexpression of $\alpha_v\beta_3$ integrin under NIR laser irradiation. The "smart" nanoprobes bound with the inner walls of tumor vessels, can absorb the optical energy from NIR laser irradiation, transfer into thermal energy, and kill tumor cells, which led to the extended lifespan of mice in the test group. Interestingly, we observed that tumors in four mice completely disappeared, which indirectly suggests that prepared RGD-dGNR nanoprobes own great potential in tumor selective therapy; further study will focus on investigating the optimal therapeutic condition of RGD-dGNR nanoprobes for killing tumor cells in animal model loaded with tumor.

So far gold nanorod-based photothermal therapy has been actively investigated. For example, El-Sayed et al.[9] conjugated GNRs to anti-EGFR monoclonal antibodies (many solid tumors overexpress EGFR) and incubated them in a nonmalignant epithelial cell and two malignant oral epithelial cell lines. The anti-EGFR/GNRs themselves were not cytotoxic and destroyed the tumor cells without harming healthy cells after light irradiation. Wei and co-workers[11] investigated photothermal effects of folate-conjugated GNRs to KB cells. With the help of real-time TPL microscopy, they found that photothermolysis of KB cells was particularly effective when folate-GNRs were localized on the cell membrane following fs-pulsed excitation. Folate-GNR-mediated cavitation disrupted membrane integrity, leading to cell death. The mechanism is different from traditional assumptions of nanoparticle-mediated hyperthermia based on systemic temperature changes. GNR photothermal therapy was also used for fighting against pathogenic bacteria[37] and parasites.[38] In our study, we also observed that excess free RGD peptides in medium can inhibit the uptake of RGD-dGNR nanoprobes by tumor cells and vasculature endothelial cells, which highly suggests that receptor-mediated endocytosis is the main pathway of uptake of RGD-dGNR nanoprobes by melanoma A375 cells. So far some reports showed that dendrimer can form a nanoscale hole in the surface of tumor cells[39] and can improve the efficiency of uptake of dendrimer-modified nanoparticles by tumor cells. In our study, the dendrimer-based nanoscale hole endocytosis pathway may have less influence on the uptake of RGd-dGNR nanoprobes by tumor cells.

Regarding the therapeutic effects of active targeting and passive targeting based on GNRs, we also compared the difference between them. According to the distribution of dGNRs and RGD-dGNRs in the mice loaded with tumors, we can clearly observe slight or moderate dGNR accumulation in tumor tissues, indicating dGNRs can preferentially

(37) Norman, R. S.; Stone, J. W.; Gole, A.; Murphy, C. J.; Sabo-Att-Wood, T. L. Targeted Photothermal Lysis of the Pathogenic Bacteria, *Pseudomonas aeruginosa*, with Gold Nanorods. *Nano Lett.* **2008**, *8*, 302–306.

(38) Pissuwan, D.; Valenzuela, S. M.; Miller, C. M.; Cortie, M. B. Golden Bullet? Selective Targeting of Toxoplasma gondii Tachyzoites Using Antibody-Functionalized Gold Nanorods. *Nano Lett.* **2007**, *7*, 3808–3812.

(39) Mecke, A.; Uppuluri, S.; Sassanella, T. M.; Lee, D. K.; Ramamoorthy, A.; Baker, J. R., Jr.; Orr, B. G.; Banaszak Holl, M. M. Direct observation of lipid bilayer disruption by poly(amidoamine) dendrimers. *Chem. Phys. Lipids* **2004**, *132*, 3–14.

Scheme 1. Accumulation of Gold Nanorods in Tumors through Both the EPR Effect and Active Binding[a]

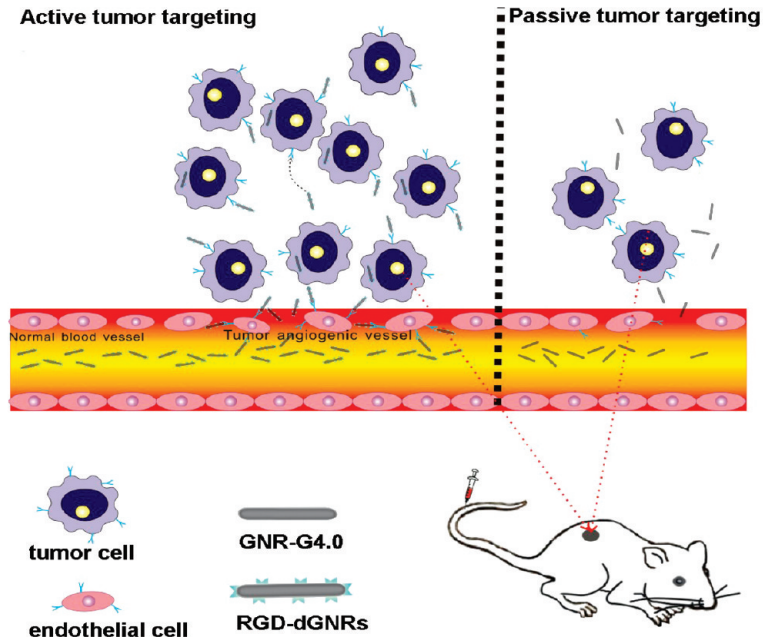

[a] Active targeting shows more specific and efficient binding ability than passive targeting. The photoactive therapy of RGD-dGNR conjugation involved in directly destroying tumor cells and destroying tumor angiogenic vessels result in cell "starvation".

accumulate into tumor tissues due to the EPR effects, but the amount of dGNRs in tumor tissues is less than that of RGD-dGNR nanoprobes in the test group. We observed that the NIR laser irradiation energy at 70 mW can effectively destroy cancer cells *in vitro*, which is lower than the threshold based on PEGylated GNRs.[9] This difference may be caused by binding of G4.0 dendrimers-GNRs with the RGD peptides via covalent bond. Although the dGNR-based passive targeting photothermal therapy can inhibit tumor growth, RGD-dGNR nanoprobe-based active targeting photothermal therapy exhibits better therapeutic effects, which are consistent with biodistribution of dGNRs and RGD-dGNRs in mice loaded with tumors. Therefore, we consider that the prepared RGD-dGNR nanoprobes may be one kind of general nanoprobe, which may be widely applied for therapy of those tumors with overexpression of $\alpha_V\beta_3$ integrin. Compared to antibody-conjugated GNRs or other nanoparticle-based therapy strategy, RGD-dGNR nanoprobes have some obvious advantages such as favorable pharmacokinetics and better tumor penetration ability due to its smaller size, less nonspecific binding to normal organs and tissues, easy fabricating and modifying.[40,41]

In our study, we used reflectance confocal microscopy to observe clearly that the blood flow inside tumor tissues in the test group began to be blocked at 3 h after NIR laser irradiation. RCM represents a novel tool to allow noninvasive imaging of the skin tumor cellular structures *in situ* and in real time. Pigment melanin and melanosomes are the strongest sources of contrast for tumor images.[42] Specifically it is suitable for the observation of melanoma lesions such as a hyperrefractive cluster of melanoma cells, and architectural disruption of the dermal−epidermal junction in the animal models, and the observation of blood flow status in the tumor tissues. RCM may be an ideal noninvasive tool for monitoring therapeutic effects of anticancer agents on superficial cancer.

Based on those data mentioned above, we suggest the possible therapeutic mechanism as follows: (1) the prepared "smart" RGD-dGNR nanoprobes distribute rapidly into whole body of mice with tumors via the circulatory system, and mainly enter into liver and tumor vessels; (2) "smart" nanoprobes bind with the $\alpha_V\beta_3$ integrins on the surface of melanoma A735 cells and inner walls of tumor vessels, and enter into cytoplasm via receptor-mediated endocytosis pathway; (3) under NIR laser irradiation, the RGD-dGNR nanoprobes absorb NIR laser and transfer laser energy into heat, damaging vascular endothelial cells and blocking the blood flow in tumor vessels, which inhibits the newborn vessels in tumor tissues, block supply chains of nutrients and oxygen, "starve" tumor cells, and finally result in the necrosis or disappearance of tumor tissues (Scheme 1).

In conclusion, our study confirms that the RGD-conjugated dGNR nanoprobes are not cytotoxic, can specifically target tumor cells and vascular cells inside tumor tissues, and exhibit selective destructive effects on the melanoma cells

(40) Aina, O.; Sroka, T.; Chen, M.; Lam, K. Therapeutic cancer targeting peptides. *Biopolymers* **2002**, *66*, 184–199.

(41) Okarvi, S. Peptide-based radiopharmaceuticals: future tools for diagnostic imaging of cancers and other diseases. *Med. Res. Rev.* **2004**, *24*, 357–397.

(42) Rajadhyaksha, M.; Grossman, M.; Esterowitz, D.; Webb, R.; Anderson, R. In vivo confocal scanning laser microscopy of human skin: melanin provides strong contrast. *J. Invest. Dermatol.* **1995**, *104*, 946–952.

under NIR laser irradiation. They can even make part of the tumor tissues in mice disappear. Compared with presently available reports, the RGD-dGNR nanoprobe-based targeting therapy possesses some major advantages, which can extend to various tumors with overexpressed $\alpha_V\beta_3$ integrins. The RGD-dGNR-based therapy strategy has great potential in applications such as tumor targeting imaging and selective photothermal therapy.

Acknowledgment. This work is supported by China National 973 Projects (No. 2005CB723400-G, No. 2010CB933900), China National 863 Project (No. 2007AA022004), China Key project (2009ZX10004-311), China Natural Scientific Fund (No. 20471599 and No. 30672147), Wenzhou Fund of Science and Technology (No. 20070034).

Supporting Information Available: Supplementary Figures 1−8 and Supplementary Video 1 (including two video files) as described in the text. This material is available free of charge via the Internet at http://pubs.acs.org.

MP9001415